A Novel Quantum Orthogonal Frequency-Division Multiplexing Transmission Scheme

Mohammed R. Almasaoodi[1, 2], Abdulbasit M. A. Sabaawi[1, 3], Sara El Gaily[1], Sándor Imre[1]
Department of Networked Systems and Services, Faculty of Electrical Engineering, and Informatics,
Budapest University of Technology and Economics, Budapest, Hungary[1]
Kerbala University, Kerbala, Iraq[2]
College of Electronics Engineering, Ninevah University, Mosul, Iraq[3]

***Abstract*—Recently, extensive research attention has been dedicated to enabling Orthogonal Frequency-Division Multiplexing (OFDM) waveforms to be compatible with a modern communication system. Encoding data as OFDM wavelengths still has a lot of problems, like the peak-to-average power ratio (PAPR) and the cyclic prefix (CP), which are important factors that affect how efficiently the spectrum is used. To meet the quality-of-service requirements imposed by communication system applications, this paper proposes to replace the classical encoding and decoding schemes, classical channel, discrete Fourier transform (DFT), and inverse discrete Fourier transform (IDFT) with their classical counterparts. This new quantum OFDM transmission scheme allows for the preparation of a quantum OFDM symbol without the need to incorporate a CP. To validate the accuracy of the suggested quantum OFDM transmission scheme, we compared it with the most widely recognised reference quantum transmission scheme. We have demonstrated that increasing the channel resistivity results in a higher probability of correctly measuring the quantum state in the quantum OFDM transmission scheme compared to the reference quantum transmission scheme. The results are verified by IBM's Qiskit.**

Keywords*—Discrete Fourier transform; quantum Fourier transform; orthogonal frequency-division multiplexing; quantum channel

I. Introduction

Wireless communication has seen substantial growth, particularly in Internet of Things (IoT) applications. The analysis highlights the prevalence of end-to-end packet delays in IoT communications [1], and emphasizes the need for energy-efficient strategies in task allocation [2]. The advent of 5G technology promises to transform connectivity with speeds up to 20 Gbps, enhancing transmissions and reducing latency for applications like IoT robotic surgery and smart education platforms [3]–[5]. Moreover, advancements in multimedia transmission [6] and sensor networks for precision agriculture [7] demonstrate the broad impact of robust wireless technologies across various sectors.

Orthogonal Frequency-Division Multiplexing (OFDM) technology has been extensively employed in data transmission for 4G wireless communication networks. OFDM is a multicarrier orthogonal digital communication scheme [8]. The binary data is encoded into symbols using one of the digital modulation schemes [9], and the modulated symbols are loaded over carrier frequencies. The available channel bandwidth is divided into bands that are called frequency subcarriers, where each one is exploited for transmitting modulated symbols. The OFDM technology allows more data transmission, overlapping multiple sub-channels, and reduces inter-symbol interference (ISI) and inter-carrier interference (ICI) [10], thanks to the non-overlapping transmitted orthogonal signals. One significant benefit of the OFDM in comparison to single-carrier schemes lies in its notable spectral efficiency, resilience against multipath fading, and adaptability to varying channel circumstances [11]. Implementing OFDM for 5G systems faces challenges like inter-carrier interference and high peak-to-average power ratios [12]. Additionally, IoT applications require waveforms with sub-millisecond latencies, further driving advancements in OFDM technology [13].

The successful reception of a transmitted signal over a wireless channel can be challenging due to ISI and ICI. To address these issues, the technique of incorporating a cyclic prefix (CP) into OFDM symbols is commonly employed. Although this addition of a cyclic prefix helps to mitigate the effects of multipath fading and carrier interference. The CP consumes a portion of the available spectrum, which reduces the overall spectral efficiency and increases the latency of the transmission system. There are many techniques used to reduce CP in an OFDM system, like reducing CP by shortening the effective channel impulse response using a time-domain equaliser [14] or a frequency-domain equaliser as in [15]. In [16], the authors introduced a method based on the concept of multiple symbol encapsulation to reduce CP.

Quantum communication harnesses the quantum nature of information, providing a dependable solution for achieving high transmission bit rates and secure communication channels over long distances [17], [18]. Moreover, these systems possess the capability to transmit significantly more data than traditional binary-based systems _ quantum channels can carry more information than classical ones thanks to the quantum superposition principal_, executing computational tasks exponentially faster than their classical counterparts [19]–[21].

The Quantum Fourier Transform (QFT) and its Inverse (IQFT) are used by Quantum Orthogonal Frequency-Division Multiplexing (Q-OFDM) to send and receive data through quantum communication channels. The QFT is a crucial element within the framework of quantum algorithms, signifying its pivotal role in advancing quantum computing technology [22].

Many academic studies have emphasized the crucial role played by the QFT and quantum simulation in advancing the

area of quantum computing. The authors in [23] present new methods for implementing QFT circuits on quantum hardware. In larger systems, they use program synthesis to manage these circuits more efficiently, simplifying operations and reducing complexity. Their approach improves the practical use of QFT in quantum computing by optimizing circuit layouts for enhanced performance. The study in [24] describes a multi-user quantum communication system that combines Code Division Multiple Access (CDMA) with QFT and IQFT. This approach enhances scalability and security, allowing multiple users to communicate simultaneously while protecting against eavesdropping. The authors in [25] improved the Quantum Phase Estimation (QPE) algorithm by optimizing QFT and IQFT. This enhancement reduces the circuit depth and error rates, resulting in higher accuracy and efficiency in QPE. They demonstrate notable advancements by comparing their method with current implementations, underscoring the importance of optimized QFT and IQFT in effective quantum computing applications.

This paper proposes a novel quantum OFDM transmission scheme for communication system. The quantum OFDM symbol will allow more data transmission compared to its classical counterpart, thanks to the quantum superposition concept, as well as high transmission speed due to exploiting the embedded quantum entanglement states in the quantum OFDM signal. Moreover, the quantum OFDM scheme offers a low computational complexity compared to its classical counterpart due to the use of the quantum Fourier transform (QFT) and the inverse quantum Fourier transform (IQFT) as signal multiplexing methods. To the best of our knowledge, there is no existing research addressing the challenges posed by the OFDM waveform in using quantum communication systems.

In our study, we employed various rotation gates, including $R_x(\theta_t)$, $R_y(\theta_t)$, and $R_z(\theta_t)$, as quantum channels to simulate different forms of quantum noise and decoherence. These gates are instrumental in modifying the state of qubits by adjusting their phase or amplitude, thereby replicating the real-world impact of quantum channels on the transmission of quantum information. However, the $R_z(\theta_t)$ gate was omitted from our simulation because phase shifts do not influence the measurements employed in our model.

This paper is organized as follows; Section II provides a detailed classical OFDM transmission model implemented using IDFT/DFT. This model is extended in detail in Section III, to the quantum version. In Section IV, to validate the accuracy of the suggested quantum OFDM transmission scheme, we compared it with the most widely recognized reference quantum transmission scheme. Finally, Section V concludes the manuscript.

II. Classical Orthogonal Frequency-Division Multiplexing Transmission System

The classical OFDM transmission scheme primarily comprises the following components: encoder and decoder, serial-to-parallel (S/P) and parallel-to-serial (P/S) modules, the IDFT and DFT processes, cyclic prefix blocks, and the channel. The architecture of the OFDM transmission implemented using IDFT/DFT is depicted in Fig. 1.

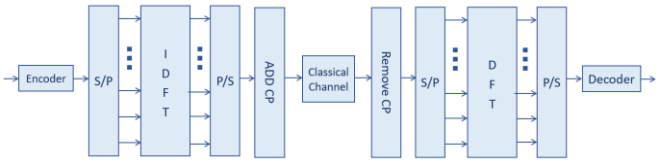

Fig. 1. Classical OFDM transmission system implemented using IDFT/DFT.

Let's consider the message bits $M = a_1 \dots a_m$. The encoder of the OFDM transmitter encoded the message bits M into M-quadrature amplitude modulation (M-QAM) or phase shift keying (PSK) symbol. Assuming that the message bits M is converted into N symbols. The serial data symbols N are converted into the parallel stream using S/P module. Next, each k^{th} symbol $X[k]$ is loaded into a different subcarrier. It is interesting to note that this study assumes that the number of symbols equals the number of subcarriers of the OFDM signal.

One writes the n^{th} transmitted time domain sample generated using IDFT process as,

$$x[n] = IDFT(X[k]) = \sum_{k=0}^{N-1} X[k] e^{j2\pi kn/N} \text{ for } n = 0,1, \dots, N-1 \quad (1)$$

It is important to mention that each n^{th} discrete time OFDM symbol $x[n]$ carry information about the overall remaining transmitted symbols. To mitigate the effect of multipath fading, the cyclic prefix is added to the obtained OFDM symbol. This is accomplished by copying the last samples from the end of the OFDM symbol and appending them to the beginning. It is worth mentioning that the proposed OFDM transmission system considers the effect of the channel while neglecting the influence of noise.

Let $y[n]$ be the n^{th} received time domain sample of the received OFDM symbol. One expresses $y[n]$ as,

$$y[n] = h[n] * x[n] \quad (2)$$

where $h[n]$ refers to the discrete time impulse response of the channel. At the OFDM receiver side, one calculates the DFT of $y[n]$ as follows,

$$Y[k] = DFT(y[n]) \quad (3)$$

where, $Y[k]$ denotes the k^{th} subcarrier frequency component of the received symbol. One can verify that $Y[k]$ can be expressed as,

$$Y[k] = \sum_{n=0}^{N-1} y[n] e^{-j2\pi kn/N} = H[k].X[k] \quad (4)$$

where $H[k]$ represents the k^{th} subcarrier frequency component of the channel frequency response. It is worth noting that the equality in (4) holds true if and only if the cyclic prefix is incorporated into the OFDM symbol.

III. Quantum Orthogonal Frequency-Division Multiplexing Transmission System

In the quantum analogue of the classical OFDM transmission system presented in Section II, the components of the quantum OFDM transmission scheme and data representation are entirely distinct. The functionalities of the quantum OFDM transmission are categorized into the following blocks: quantum encoder and decoder (or measurement device), serial-to-parallel and parallel-to-serial modules, IQFT and QFT processes, and the quantum channel. The quantum OFDM transmission architecture implemented using IQFT/QFT is illustrated in Fig. 2.

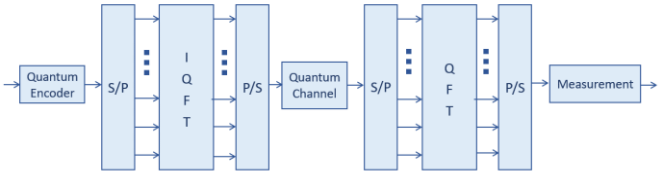

Fig. 2. Quantum OFDM transmission system implemented using IQFT/QFT.

In quantum computing and communication, quantum encoding stands in stark contrast to any classical counterpart scheme [26]. Quantum encoding involves the preparation of quantum states. Similarly, the decoding process revolves around the measurement of the received quantum system. Furthermore, the quantum channel encompasses a broader and more generalised form compared to its classical counterpart.

Let start by introducing the operational principle of the quantum encoder. In this context, the message bits M undergo encoding into a quantum state of m qubits as follows,

$$|\psi_{enc}\rangle = \sum_{i=0}^{N'-1} \psi_i |i\rangle, \tag{5}$$

where ψ_i refers to the probability amplitude of the computational basis state $|i\rangle$, while N' denotes the overall number of possible combinations of m bits, such that $N' = 2^m$. It is worth noting that the complete set of message bits M, is stored within a single quantum register of size equal to $log_2(M)$. Let us name $|\psi_{enc}\rangle$ as the modulated quantum message/register.

At this juncture, we can apply the IQFT transformation _denoted by F^{-1}_ to the prepared modulated quantum message, thereby generating the quantum equivalent of the classical OFDM symbol. One expresses the quantum OFDM symbol as,

$$|\varphi_{trans}\rangle = F^{-1}|\psi_{enc}\rangle, \tag{6}$$

such that,

$$|\varphi_{trans}\rangle = \sum_{l=0}^{N'-1} \varphi_l |l\rangle. \tag{7}$$

The IQFT transformation _denoted by F^{-1}_ exclusively impacts the computational basis states of $|\psi_{enc}\rangle$, implying that the IDFT leaves the probability amplitudes of the quantum state $|\psi_{enc}\rangle$ unaffected. One can write,

$$\varphi_l = \frac{1}{\sqrt{N'}} \sum_{i=0}^{N'-1} \psi_i \, e^{-j\frac{2\pi i l}{N'}} \tag{8}$$

and

$$F^{-1}|i\rangle = \frac{1}{\sqrt{N'}} \sum_{l=0}^{N'-1} e^{-j\frac{2\pi i l}{N'}} |l\rangle. \tag{9}$$

It is straightforward to verify that,

$$F^{-1}|i\rangle = \frac{1}{\sqrt{N'}} \bigotimes_{t=1}^{m} \left(|0\rangle + e^{-j\frac{2\pi i}{2^t}}|1\rangle\right). \tag{10}$$

Modelling the impact of the quantum channel is achievable through a unitary operator, as it preserves the input quantum state and avoids information loss. To this end, we opt to implement a single-qubit gate known as the rotation operator. We consider $R_x(\theta_t)$ or $R_y(\theta_t)$ as a quantum channel model [27],

$$R_x(\theta_t) = \begin{bmatrix} \cos\left(\frac{\theta_t}{2}\right) & -i.\sin\left(\frac{\theta_t}{2}\right) \\ -i.\sin\left(\frac{\theta_t}{2}\right) & \cos\left(\frac{\theta_t}{2}\right) \end{bmatrix}$$

$$or \tag{11}$$

$$R_y(\theta_t) = \begin{bmatrix} \cos\left(\frac{\theta_t}{2}\right) & -\sin\left(\frac{\theta_t}{2}\right) \\ \sin\left(\frac{\theta_t}{2}\right) & \cos\left(\frac{\theta_t}{2}\right) \end{bmatrix}$$

where θ_t represents the rotation angle, it serves as an indicator of the noise level in the quantum channel. A large value of θ_t indicates a high level of noise in the quantum channel. Due to the entanglement of the quantum components within the quantum OFDM symbol $|\varphi_{trans}\rangle$, applying a single qubit phase gate to each individual qubit becomes unfeasible. To address this, we approached the situation by conceptualizing the entirety of quantum channels as a single global quantum channel that influences the quantum OFDM symbol. Let $P_t = R_y(\theta_t)$ or $P_t = R_x(\theta_t)$. One describes the global quantum channel as,

$$P = \bigotimes_{t=1}^{m} P_t. \tag{12}$$

It is important to highlight that our proposed quantum OFDM transmission system does not account for the influence of the environment quantum state.

On the quantum OFDM receiver side, the received quantum OFDM symbol can be described as,

$$|\varphi_{recei}\rangle = PF^{-1}|\psi_{enc}\rangle. \tag{13}$$

Applying the QFT transformation _denoted by F _ on $|\varphi_{recei}>$, one obtains,

$$|\psi_{dec}\rangle = F|\varphi_{recei}\rangle. \quad (14)$$

Finally, the classical decoder is replaced by a measurement device that converts the acquired quantum state back to its original classical form. It is worth noting that employing a quantum OFDM transmission system makes it possible to do away with the need for a cyclic prefix. This is due to the inherent interaction of quantum states without interference in nature.

IV. Simulation Results

In this section, we showcase the efficiency of the quantum OFDM transmission scheme by comparing it to a reference quantum transmission scheme in terms of the probability of measuring the correct transmitted quantum state. The results have been validated through extensive simulations using the Qiskit platform.

The simulation setup for the quantum OFDM transmission scheme involves a four-qubit input quantum state connected to the IQFT process, followed by a rotation operator representing the channel effect, and then a QFT process. The final step includes a measurement device. Fig. 3 the quantum OFDM transmission scheme.

The simulation setup for the reference quantum transmission scheme includes a four-qubit input quantum state connected to rotation operators representing the channel effect, followed by a measurement device. Fig. 4 presents the reference quantum transmission scheme.

The message bits $M = 4$ undergo encoding into a quantum input state, where, for example, 0000 is represented as $|0000\rangle$ and 0001 is represented as $|0001\rangle$, etc. The input quantum states of the quantum circuits, either the quantum OFDM transmission scheme circuit or the reference transmission scheme, are randomly selected from the set of all possible quantum states, which is equal to 2^4. Subsequently, the generated quantum state undergoes processing by the IQFT component. Afterward, the resulting quantum state traverses the quantum channel, which is modelled by rotation operators $R_x(\theta_t)$ or $R_y(\theta_t)$. Following the channel, a QFT operation is applied to the received quantum state, and a measurement is performed. Fig. 5 represents in detail the components of the processes of the QFT, IQFT, and quantum channel. Where, The Hadamard gates H are employed to generate superpositions, and the phase gates P are used to add specific phase differences that depend on the control qubits' states in the QFT-IQFT implementation.

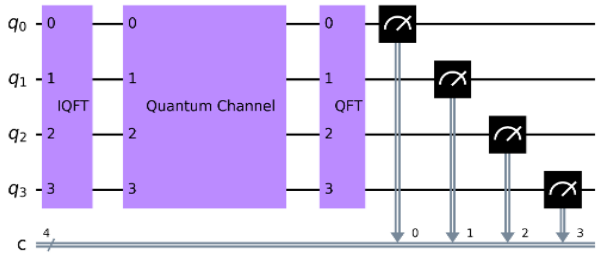

Fig. 3. Quantum OFDM transmission system implemented using Qiskit.

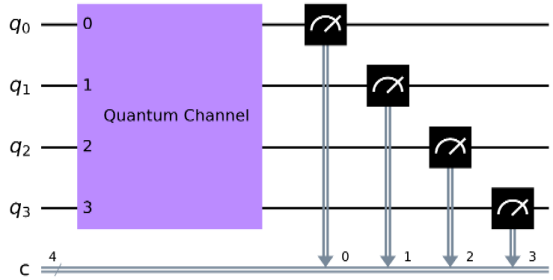

Fig. 4. Reference quantum transmission system implemented using Qiskit.

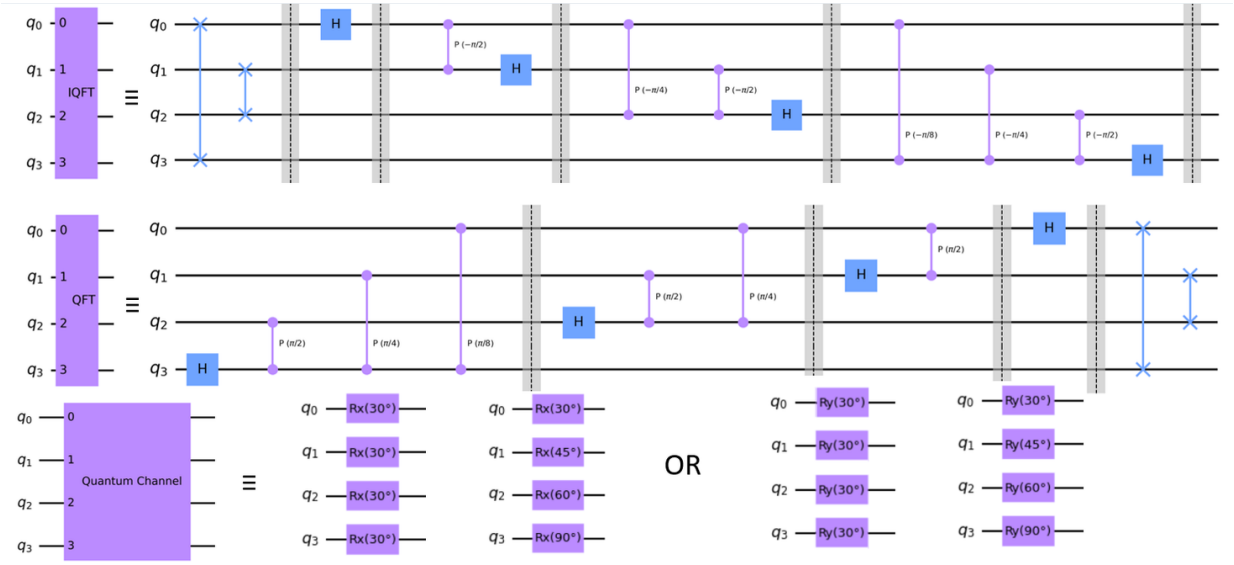

Fig. 5. Detailed components of QFT, IQFT, and quantum channel processes.

The aim is to prove that although the resistance of the quantum channel, i.e., the high level of noise in the channel, the quantum OFDM transmission scheme circuit outperforms the reference transmission scheme in terms of measuring the correct transmitted quantum state. Furthermore, the procedure is iterated for a specific number of shots (1024) to collect statistical information. For this sake, two different experiments were conducted,

- The first experiment selects random quantum input states and applies both quantum transmission schemes, i.e. the quantum OFDM transmission scheme circuit or the reference transmission scheme. The quantum channel is modelled by rotation operators $R_x(\theta_t)$, different values of the parameter θ_t are considered.
- The second experiment selects random quantum input states and applied both quantum transmission schemes. The quantum channel is modelled by rotation operators $R_y(\theta_t)$, and different values of the parameter θ_t are taken into consideration.

A. Experiment 1

The objective of this experiment is to evaluate the efficacy of the quantum OFDM transmission scheme in comparison to the reference quantum transmission scheme.

In this experiment, we employ the $R_x(\theta_t)$ rotation. This configuration of rotation is depicted in a quantum circuit as a sequence of $R_x(\theta_t)$ gates applied to each qubit, with the rotation angles θ_t explicitly set for each one. For instance, q_0, q_1, q_2, and q_3, undergo R_x rotation at angles of 30, 45, 60, and 90 degrees, respectively, accompanied by randomly generated quantum input states. Subsequently, we measured the probability in terms of the number of counts, which represents the number of times the corresponding outcome was observed. The results, including the measured probability of the correct transmitted quantum state for each quantum input state, are illustrated in Fig. 6.

Fig. 6 compares the outcomes of experiments (a), (b), and (c) for two different quantum transmission schemes: the reference quantum transmission scheme and the quantum OFDM transmission scheme. The histograms display the counts, which represent the number of times each quantum state was correctly decoded after transmission.

In subfigure (a), for the quantum OFDM scheme, the decoded state '0011' was correctly observed 698 times out of a total of 1024 transmissions, illustrating a high reliability for this state within this scheme. Conversely, the reference scheme yielded 315 counts for the same input state, indicating a lower transmission accuracy for '0011' compared to the quantum OFDM scheme.

Furthermore, the reference scheme shows a notable count for the state '1011', which suggests that there may be a distortion or error in the transmission process, as this state exhibits a similar count to '0011', which could indicate a pattern of systematic error or a bias in the quantum channel affecting these states.

As we progress to subfigures (b) and (c), we observe consistent trends with certain states showing a higher number of counts, suggesting that these states are being decoded correctly more often in one scheme over the other. For instance, in (b), the state '1011' in the quantum OFDM scheme again stands out with 653 counts, whereas in the reference scheme, which has 292 counts, the states '1011' and '0011' are more prominent. In (c), the quantum OFDM scheme exhibits an overwhelming count of 1024 for the state '0000', which is a stark contrast to the more evenly distributed counts across different states in the reference scheme.

These results demonstrate distinct differences in the reliability and accuracy of quantum state transmission between the reference and quantum OFDM schemes, with the latter showing a tendency to favor certain states over others. This could point to specific characteristics of the quantum OFDM scheme that may be optimised for improved performance and fidelity in quantum communication systems.

Next, we randomly generated quantum input states and maintained identical values of θ_t for all four $R_x(\theta_t)$ gates. In other words, we standardize the rotation across all qubits. The quantum circuit configuration employs a uniform sequence of R_x gates where each qubit, q_0, q_1, q_2, and q_3, is subjected to a R_x rotation of fixed degree.

We conducted multiple simulations using different values of θ_t and measured the probability of the correct transmitted quantum state. The results, including the measured probability of the correct transmitted quantum state for various values of θ_t, are presented in Table I. The resistance degree of the quantum channel increases as the parameter θ_t rises. As shown in Table I, even as the noise in the quantum channel increases, corresponding to an increased channel resistivity, the quantum OFDM transmission scheme exhibits a higher probability of correctly measuring the quantum state compared to the reference quantum transmission scheme.

B. Experiment 2

In the current experiment, we utilise the R_y rotation. This rotational configuration is represented in a quantum circuit by a sequence of $R_y(\theta_t)$ gates applied to individual qubits, with predetermined rotational angles θ_t for each qubit. Specifically, qubits q_0, q_1, q_2, and q_3 are subjected to R_y rotations at angles of 30, 45, 60, and 90 degrees, respectively, alongside quantum input states generated randomly. Following this, we evaluated the probability based on the count metric, which indicates the number of occurrences for the anticipated outcome. Fig. 7 elucidates the probabilities of accurately transmitted quantum states for each input state as measured in the experiment.

Fig. 7 exhibits a comparative statistical analysis between the reference quantum transmission scheme and the quantum OFDM transmission scheme, encapsulated in subfigures (a), (b), and (c). The histograms plot the counts, which denote the observed number of the correct transmitted states.

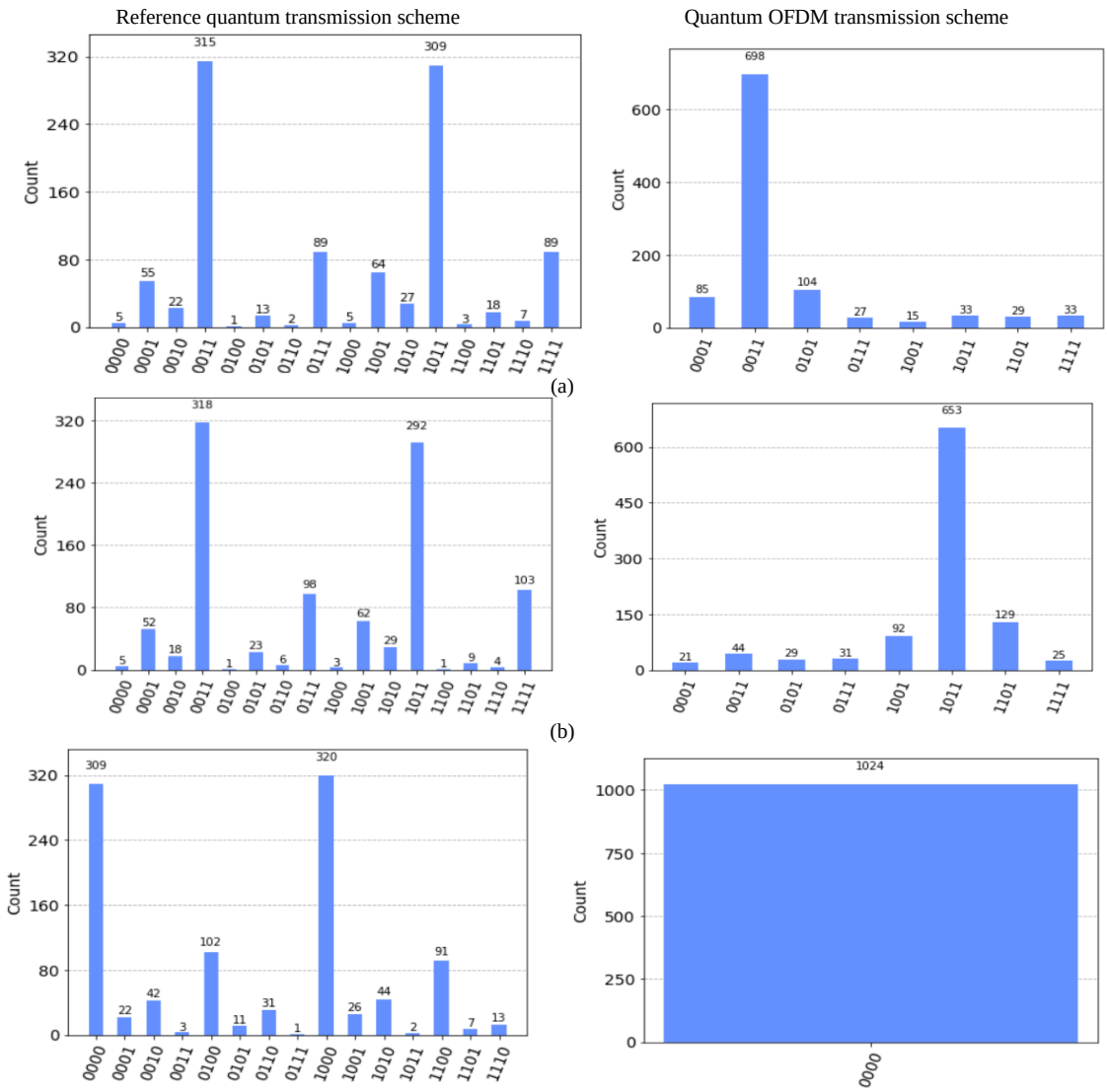

Fig. 6. The measured probability of the correct transmitted quantum state for each quantum input state by the quantum OFDM transmission scheme and the reference quantum one, the quantum channel is modelled by $R_x(\theta_t)$.

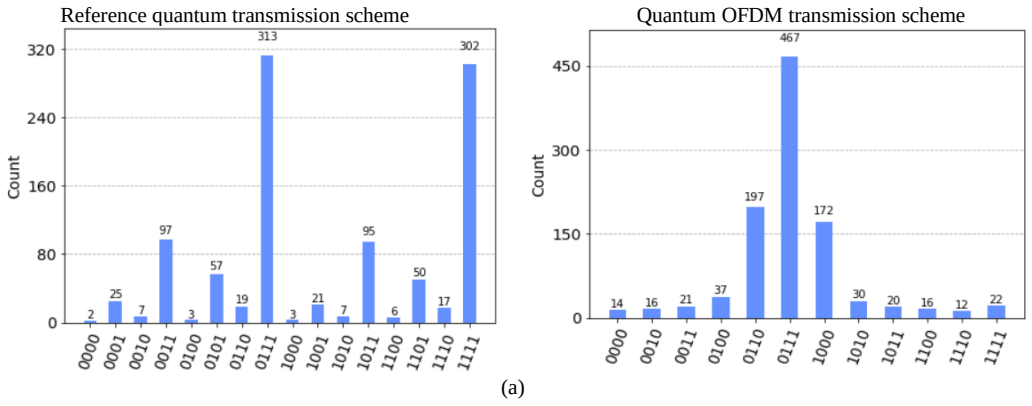

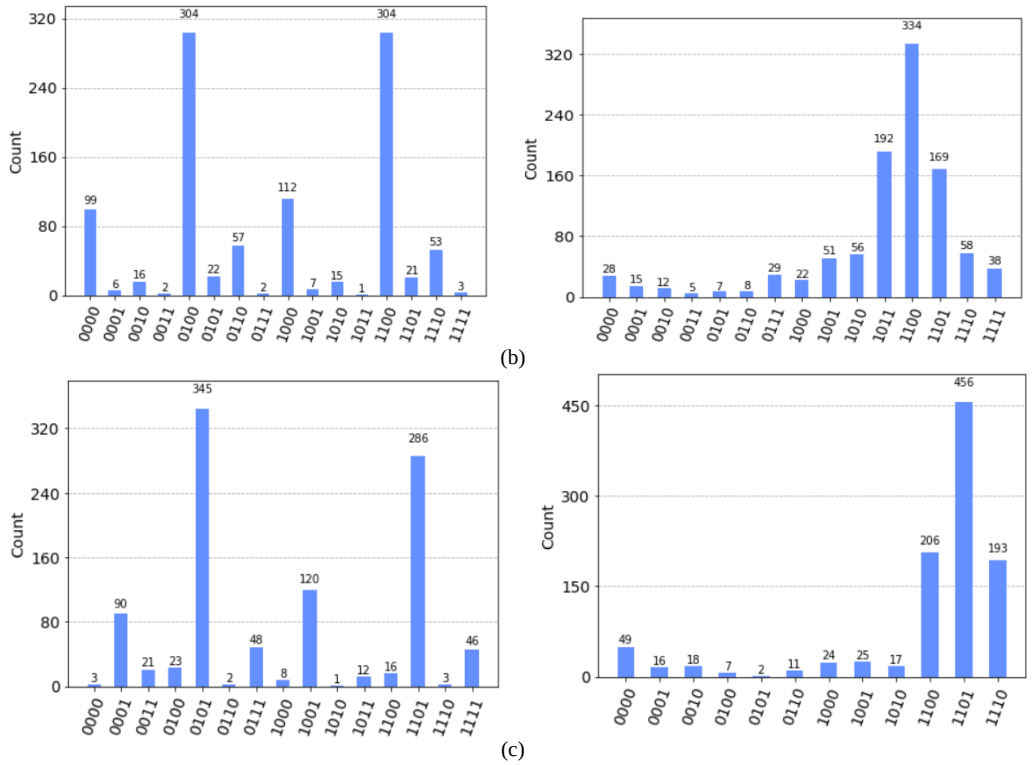

(b)

(c)

Fig. 7. The measured probability of the correct transmitted quantum state for each quantum input state by the quantum OFDM transmission scheme and the reference quantum one, the quantum channel is modelled by $R_y(\theta_t)$.

In subfigure (a), the reference scheme predominantly correctly decodes the quantum state '0111' with a count of 313. However, the high count for state '1111' appears to be an error or distortion, as this outcome is inconsistent with the input. The Quantum OFDM scheme, on the other hand, predominantly decodes state '0011' correctly, with a count of 467, and displays a Gaussian-like distribution of counts, indicating a higher fidelity in transmission for this state.

Subfigure (b) shows that the reference scheme yields the highest counts for states '0010' and '1100', with counts of 304 each, suggesting these are the most reliably transmitted states in this scheme. However, the quantum OFDM scheme again shows peaking at state '1100' with 334 counts.

In subfigure (c), an anomaly in the reference scheme is evident where the intended quantum state '1101' is recorded 286 times, yet an incorrect state '0101' appears with a higher count of 345, indicating a potential error in transmission or decoding. This suggests that the state '0101' may be a distorted version of '1101', caused by errors within the reference transmission scheme. In contrast, the Quantum OFDM scheme shows a pronounced peak at state '1101' with 456 counts, which points to a Gaussian-like distribution centred around this state, hinting at a more consistent and stable transmission characteristic.

Next, we generated quantum input states at random and maintained the same θ_t values for all four $R_y(\theta_t)$ gates. The circuit design utilises a consistent series of $R_y(\theta_t)$ gates, each imparting a rotation of a fixed degree to qubits q_0, q_1, q_2, and q_3. We ran multiple simulations with varying values of θ_t and measured the probability of the correct quantum state being transmitted.

TABLE I. THE MEASURED PROBABILITY OF CORRECTLY DECODING THE QUANTUM STATE IS EVALUATED FOR VARIOUS VALUES OF θ_t IN BOTH THE QUANTUM OFDM TRANSMISSION AND QUANTUM REFERENCE TRANSMISSION SCHEMES (THE CHANNEL IS MODELLED BY $R_x(\theta_t)$).

θ_t	Input quantum state	Quantum OFDM	Quantum Reference
20	1101	963	902
30	1011	889	776
40	0111	829	618
50	0011	642	453
60	0101	555	350
70	1001	528	221
80	1111	440	137

Table II displays the outcomes, including the measured probability of measuring the correct transmitted quantum state for various values of the parameter θ_t. As the parameter θ_t raises, the quantum channel's resistance increases. As demonstrated in Table II, the quantum OFDM transmission scheme has a greater probability of accurately measuring the quantum state than the reference quantum transmission scheme.

Building on these encouraging results, we plan to expand our research to explore the integration of the Quantum OFDM scheme into a more complex quantum massive MIMO-OFDM framework. This next phase of our research will utilize findings from our previous studies [28]–[36] to inform the development

and optimization of the scheme in a broader context. Additionally, we aim to demonstrate the theoretical advancements through extensive simulations, thereby not only validating our approach but also assessing its scalability and efficacy in more robust quantum communication environments.

TABLE II. THE MEASURED PROBABILITY OF CORRECTLY DECODING THE QUANTUM STATE IS EVALUATED FOR VARIOUS VALUES OF θ_t IN BOTH THE QUANTUM OFDM TRANSMISSION AND QUANTUM REFERENCE TRANSMISSION SCHEMES (THE CHANNEL IS MODELLED BY $R_y(\theta_t)$)

θ_t	Input quantum state	Quantum OFDM	Quantum Reference
20	0000	909	889
30	0010	842	769
40	1010	765	631
50	0001	621	513
60	0110	515	334
70	1100	313	207
80	1110	270	135

V. CONCLUSION

We propose a novel quantum OFDM transmission scheme that eliminates the need for a cyclic prefix. The results of our comparative study accentuate the enhanced efficacy of the Quantum OFDM transmission scheme over the conventional reference quantum transmission scheme. Notably, when utilizing Rx rotations, the Quantum OFDM scheme consistently delivered a higher accuracy in quantum state transmission, indicating its robustness and potential for reliable quantum communication. In contrast, the use of Ry rotations revealed a Gaussian-like distribution of state counts, signifying a predictable and systematic error pattern, which, despite the presence of noise, offers a semblance of reliability and predictability.

The reference transmission scheme, however, exhibited a random distribution of counts with pronounced peaks at incorrect states, reflecting a susceptibility to higher distortion and transmission errors. This stark difference in performance highlights the Quantum OFDM scheme's capacity to significantly enhance stability and fidelity within practical quantum communication systems. These results are supported by Qiskit platform, confirming the viability of our approach.

As we delve deeper into the implications of our findings, it is crucial to consider the inherent challenges and limitations of the proposed quantum OFDM transmission scheme outlined previously. These challenges, including quantum decoherence and noise, scalability issues, and current hardware limitations, provide essential context for our results and highlight areas for further investigation. Given these identified challenges, future research will delve into the intrinsic properties of the Quantum OFDM scheme that confer its error resilience, particularly when employing R_x rotations. An exploration into the optimal quantum encoding strategies and their influence on transmission integrity is also warranted.

ACKNOWLEDGMENT

This research was supported by the Ministry of Culture and Innovation and the National Research, Development, and Innovation Office within the Quantum Information National Laboratory of Hungary (Grant No. 2022-2.1.1-NL-2022-00004).

REFERENCES

[1] I. Maslouhi, K. Ghoumid, and K. Baibai, “Analysis of end-to-end packet delay for Internet of Things in wireless communications,” International Journal of Advanced Computer Science and Applications, vol. 9, no. 9, 2018.

[2] Y. Shan, Y. U. Renping, and J. I. N. Xin, “Whale Optimization Algorithm for Energy-Efficient Task Allocation in the Internet of Things,” International Journal of Advanced Computer Science and Applications, vol. 14, no. 10, 2023.

[3] M. A. Al-Namari, A. M. Mansoor, and M. Y. I. Idris, “A brief survey on 5G wireless mobile network,” International Journal of Advanced Computer Science and Applications, vol. 8, no. 11, 2017.

[4] A. M. Ghaleb, A. M. Mansoor, and A. Rodina, “An Energy-Efficient User-Centric Approach for High-Capacity 5G Heterogeneous Cellular Networks,” International Journal of Advanced Computer Science and Applications, vol. 9, no. 1, 2018.

[5] D. K. Dake and B. A. Ofosu, “5G enabled technologies for smart education,” International journal of advanced computer science and applications, vol. 10, no. 12, 2019.

[6] M. Shwetha, “Multimedia Transmission Mechanism for Streaming Over Wireless Communication Channel,” International Journal of Advanced Computer Science and Applications, vol. 12, no. 9, 2021.

[7] F. Kiani and A. Seyyedabbasi, “Wireless sensor network and internet of things in precision agriculture,” International Journal of Advanced Computer Science and Applications, 2018.

[8] K. P. Nagapushpa and K. N. Chitra, “Studying applicability feasibility of OFDM in upcoming 5G network,” International Journal of Advanced Computer Science and Applications, vol. 8, no. 1, 2017.

[9] S. Gupta and A. Goel, “Improved selected mapping technique for reduction of papr in ofdm systems,” International Journal of Advanced Computer Science and Applications, vol. 11, no. 10, 2020.

[10] M. Masud and Md. Kamal, “Adaptive Channel Estimation Techniques for MIMO OFDM Systems,” International Journal of Advanced Computer Science and Applications, vol. 1, no. 6, 2010, doi: 10.14569/IJACSA.2010.010620.

[11] R. Prasad, OFDM for wireless communications systems. Artech House, 2004.

[12] G. Z. Islam and M. A. Kashem, “An OFDMA-based Hybrid MAC Protocol for IEEE 802.11ax,” Infocommunications journal, no. 2, pp. 48–57, 2019, doi: 10.36244/ICJ.2019.2.6.

[13] H. Harkat, P. Monteiro, A. Gameiro, F. Guiomar, and H. Farhana Thariq Ahmed, “A survey on MIMO-OFDM systems: review of recent trends,” Signals, vol. 3, no. 2, pp. 359–395, 2022.

[14] A. Hamdan, H. Hijazi, L. Ros, A. Al-Ghouwayel, and C. Siclet, “Equalization with Time Domain Preprocessing for OFDM and FBMC in Flat Fading Fast Varying Channels,” in 2022 IEEE 6th International Symposium on Telecommunication Technologies (ISTT), IEEE, 2022, pp. 91–96.

[15] S. E. Zegrar and H. Arslan, “Common CP-OFDM transceiver design for low-complexity frequency domain equalization,” IEEE Wireless Communications Letters, vol. 11, no. 7, pp. 1349–1353, 2022.

[16] X. Wang, Y. Wu, J.-Y. Chouinard, and H.-C. Wu, “On the design and performance analysis of multisymbol encapsulated OFDM systems,” IEEE Trans Veh Technol, vol. 55, no. 3, pp. 990–1002, 2006.

[17] S. Imre and F. Balazs, Quantum Computing and Communications: an engineering approach. John Wiley & Sons, 2005.

[18] S. Imre and L. Gyongyosi, Advanced quantum communications: an engineering approach. John Wiley & Sons, 2012.

[19] S. J. Nawaz, S. K. Sharma, S. Wyne, M. N. Patwary, and M. Asaduzzaman, "Quantum machine learning for 6G communication networks: State-of-the-art and vision for the future," IEEE access, vol. 7, pp. 46317–46350, 2019.

[20] P. Botsinis et al., "Quantum search algorithms for wireless communications," IEEE Communications Surveys & Tutorials, vol. 21, no. 2, pp. 1209–1242, 2018.

[21] S. El Gaily and S. Imre, "Constrained Quantum Optimization for Resource Distribution Management," International Journal of Advanced Computer Science and Applications, vol. 12, no. 8, 2021.

[22] J. Chen, E. M. Stoudenmire, and S. R. White, "Quantum fourier transform has small entanglement," PRX Quantum, vol. 4, no. 4, p. 040318, 2023.

[23] Y. Jin et al., "Quantum Fourier Transformation Circuits Compilation," arXiv preprint arXiv:2312.16114, 2023.

[24] M. Anand and P. T. Kolusu, "A Novel Multi-User Quantum Communication System Using CDMA and Quantum Fourier Transform," in Ubiquitous Communications and Network Computing: 4th EAI International Conference, UBICNET 2021, Virtual Event, March 2021, Proceedings, Springer, 2021, pp. 79–90.

[25] H. Mohammadbagherpoor, Y.-H. Oh, P. Dreher, A. Singh, X. Yu, and A. J. Rindos, "An improved implementation approach for quantum phase estimation on quantum computers," in 2019 IEEE International Conference on Rebooting Computing (ICRC), IEEE, 2019, pp. 1–9.

[26] L. Gyongyosi, S. Imre, and H. V. Nguyen, "A survey on quantum channel capacities," IEEE Communications Surveys & Tutorials, vol. 20, no. 2, pp. 1149–1205, 2018.

[27] M. A. Nielsen and I. L. Chuang, Quantum computation and quantum information. Cambridge university press, 2010.

[28] M. R. Almasaoodi, A. M. A. Sabaawi, S. El Gaily, and S. Imre, "New Quantum Genetic Algorithm Based on Constrained Quantum Optimization," Karbala International Journal of Modern Science, vol. 9, no. 4, Oct. 2023, doi: 10.33640/2405-609X.3325.

[29] A. M. A. Sabaawi, M. R. Almasaoodi, S. El Gaily, and S. Imre, "MIMO System Based-Constrained Quantum optimization Solution," in 2022 13th International Symposium on Communication Systems, Networks and Digital Signal Processing (CSNDSP), IEEE, 2022, pp. 488–492.

[30] A. M. A. Sabaawi, M. R. Almasaoodi, S. El Gaily, and S. Imre, "New Constrained Quantum Optimization Algorithm for Power Allocation in MIMO," in 2022 45th International Conference on Telecommunications and Signal Processing (TSP), IEEE, 2022, pp. 146–149.

[31] M. Almasaoodi, A. Sabaawi, S. El Gaily, and S. Imre, "New Quantum Strategy for MIMO System Optimization," in Proceedings of the 19th International Conference on Wireless Networks and Mobile Systems, SCITEPRESS - Science and Technology Publications, 2022, pp. 61–68. doi: 10.5220/0011305100003286.

[32] M. Almasaoodi, A. Sabaawi, S. El Gaily, and S. Imre, "Power Optimization of Massive MIMO Using Quantum Genetic Algorithm," in 1st Workshop on Intelligent Infocommunication Networks, Systems and Services (WI2NS2), Budapest University of Technology and Economics, 2023, pp. 89–94.

[33] A. M. A. Sabaawi, M. R. Almasaoodi, S. El Gaily, and S. Imre, "Unconstrained Quantum Genetic Algorithm for Massive MIMO System," in 2023 17th International Conference on Telecommunications (ConTEL), IEEE, 2023, pp. 1–6.

[34] M. R. Almasaoodi, A. M. A. Sabaawi, S. El Gaily, and S. Imre, "Optimizing Energy Efficiency of MIMO Using Quantum Genetic Algorithm," in 2023 Advances in Science and Engineering Technology International Conferences (ASET), IEEE, 2023, pp. 1–6.

[35] A. Sabaawi, M. R. Almasaoodi, S. El Gaily, and S. Imre, "Quantum Genetic Algorithm for Highly Constrained Optimization Problems," Infocommunications Journal: A Publication Of The Scientific Association For Infocommunications (HTE), vol. 15, no. 3, pp. 63–71, 2023.

[36] A. M. A. Sabaawi, M. R. Almasaoodi, S. El Gaily, and S. Imre, "Energy efficiency optimisation in massive multiple - input, multiple - output network for 5G applications using new quantum genetic algorithm," IET Networks, 2023.